A Microfiber Bragg Grating Based on a Microstructured Rod: A Proposal

Fei Xu, Gilberto Brambilla, Jing Feng, and Yan-Qing Lu, *Member, IEEE*

***Abstract*—We propose a system suitable for the manufacture of microfiber gratings by wrapping a microfiber on a microstructured rod, which has large refractive index differences (deep teeth) and a large coupling coefficient. Different grating profiles can be realized by using different rod designs. This type of device has great potential for applications in future all-fiber microcircuits.**

***Index Terms*—Grating, microfiber.**

I. Introduction

MICROFIBER-BASED devices (MDs) have recently attracted much attention because of the enormous progress in the fabrication of low-loss submicrometric optical wires which allow for low-loss evanescent waveguiding. Moreover, optical microdevices fabricated from subwavelength fibers offer several prospective benefits as compared to microphotonic devices based on other principles; these include low insertion loss, complete fiber compatibility, and flexibility. Being fabricated from a single-mode fiber, MDs do not experience any input–output coupling problem. Recently, the microfiber resonator has increasingly attracted interest because of its role of basic MD. However, in free space the fabrication of microfiber resonators with high reliability is challenging due to problems of stability, degradation, and cleanness [1], [2]. Coating is an elegant way to solve these issues; yet, the determination of the coating thickness is a challenging issue because a thick coating layer will limit the sensitive evanescent field, while a thin layer does not provide an appropriate protection to the device. Consequently to the development of 3-D microcoil resonators in Teflon [3] and in low index liquid [4], a refractometric sensor based on a coated optical nanowire microcoil resonator has been investigated and demonstrated [5], [6]. Although microcoil resonators have a wealth of applications (as delay lines, narrowband and complex filtering, lasing, switching, just to cite a few), for future all-fiber microphotonic circuits, more MDs (in particular gratings) are required. Similar to gratings written in conventional fibers and waveguides, microfiber grating can have several different applications, including filters, sensors, and distributed-feedback (DFB) lasers. The standard use of photosensitivity fiber core and UV writing is inconvenient for a microfiber because of the disappearance of the germanium core during the tapering process. Alternative techniques, such as metal deposition [7], focused ion beam milling or implantation [8], and plasma etch postprocessing [9] are expensive, time-consuming, and difficult because of the expensive and complicated setup, and because of the complexity in handling and postprocessing thin microfibers.

Manuscript received August 10, 2009; revised November 18, 2009; accepted November 19, 2009. First published January 08, 2010; current version published January 27, 2010. This work was supported by the 973 Program (2010CB327803 and 2006CB921805), by the National Natural Science Foundation of China (60977039 and 10874080), and by the U.K. EPSRC under the standard research grant EP/C00504X/1. The work of G. Brambilla was supported by the Royal Society (London, U.K.) under a research fellowship. The work of F. Xu and Y.-Q. Lu supported by Program for New Century Excellent Talents in University and Changjiang Scholars Program.

F. Xu, J. Feng, and Y.-Q. Lu are with Department of Materials Science and Engineering and National Laboratory of Solid State Microstructures, Nanjing University, Nanjing 210093, China (e-mail: feixu@nju.edu.cn; jingfeng@163.com; yqlu@nju.edu.cn).

G. Brambilla is with Optoelectronics Research Centre, University of Southampton, Southampton, SO17 1BJ, U.K. (e-mail:gb2@orc.soton.ac.uk).

Color versions of one or more of the figures in this letter are available online at http://ieeexplore.ieee.org.

Digital Object Identifier 10.1109/LPT.2009.2037515

II. Schematic on the Grating

In this letter, we investigate the possibility to obtain a microfiber Bragg grating (MBG) by wrapping a microfiber on a microstructured rod. Combining current enabling technologies on microstructured optical fibers [10], [11] and microfibers [1], it is possible to induce periodical corrugations leading to the coupling between forward and backward propagating waves. This kind of device should be robust, compact, and flexible.

Lasting MBGs can be fabricated by wrapping microfibers on microstructured rods, and then coating them with low-loss polymer such as Teflon or UV375. The rod can be obtained by etching a cane used in the manufacture of microstructured fibers or it can be a thick microstructured fiber.

The final MBG structure is shown in Fig. 1(a): it is a compact and strong microdevice with some air holes arranged in a circle. Fig. 1(b) presents a possible rod cross-section. The mode propagating in the microfiber experiences refractive index corrugations because its evanescent field overlaps with the support rod where there is alternation of glass and air holes. Here we only consider one ring of air holes; the inner large hole is also filled with air and the microfiber is assumed perpendicular to the rod.

The proposed MGB structure is similar to a conventional planar grating, when a coordinate increasing along the microfiber is used. Unfolding the microfiber, the MGB can be taken as a coated microfiber on a planar substrate with periodical air-hole corrugations: the equivalent structure is shown in Fig. 1(c). Here Λ is the period between two air-holes; we assume $d_1 = 0$ to simplify calculations.

As in other Bragg gratings and DFB lasers, the MGB Bragg wavelength is expressed by $\lambda_B = 2n_{\text{eff}}\Lambda/m$, where n_{eff} is the mode effective index in the unperturbed (coiled) geometry and m is the Bragg order.

The mode field in the unperturbed waveguide geometry is not calculated from the exact solution of the propagation equations, but it is derived from the perturbed (straight) geometry using

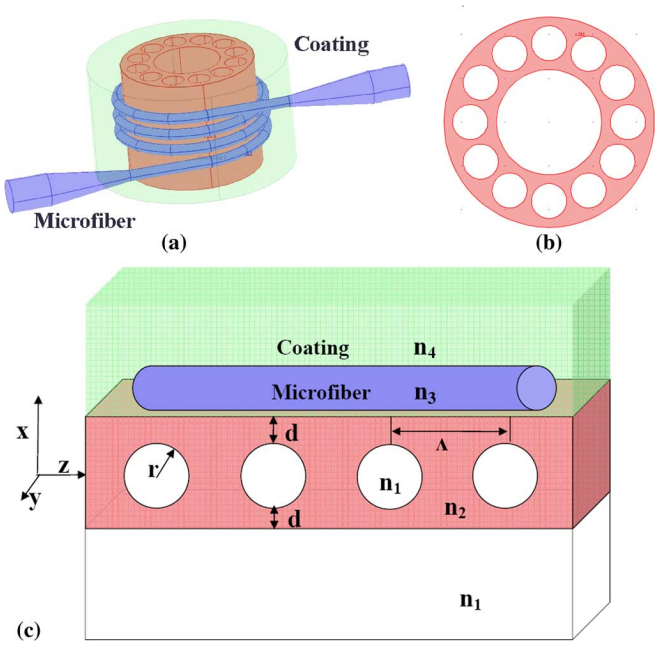

Fig. 1. (a) Schematic of the embedded MBG. (b) Cross section of the support rod; (c) the equivalent planar structure.

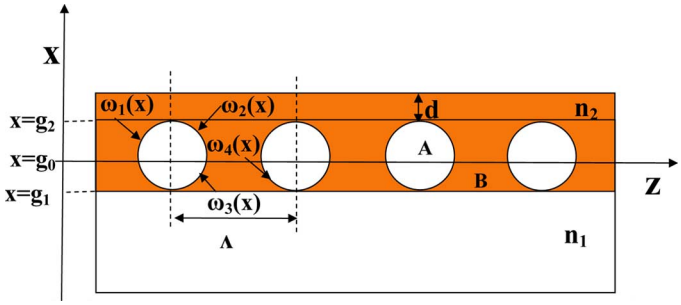

Fig. 2. Illustration of the outer layer structure of the support rod. ω_1, ω_2, ω_3, and ω_4 are the functions defining the tooth shape; g_0, g_1, and g_2 are boundaries between layers.

the method developed by Streifer: in this method, the boundary g_0 between the materials with refractive indexes n_1 (air) and n_2 (the rod material, generally silica) is shifted to compensate for the different geometry [12], [13]. g_0 is chosen to match the volume of n_1 material extending into region 2 (above g_0) to the volume of n_2 material extending into region 1 (below g_0), as shown in Fig. 2. We introduce $g_0 - g_1 = \pi r^2/\Lambda$ and effective distance d'

$$d' = g_1 + g_2 - g_0 = d + 2r - \pi r^2/\Lambda. \tag{1}$$

The functions defining the tooth shapes are $-\omega_1(x) = \omega_2(x) = \omega_3(x) = (r^2 - x^2)^{1/2}$, and $\omega_4(x) = \Lambda - (r^2 - x^2)^{1/2}$.

The propagation constant depends on d', and we can flexibly achieve chirp grating by tuning hole radii, hole pitches, or the distance between microfiber and holes. In this letter, we only discuss the uniform grating with uniform r, Λ, and d.

III. Coupling Coefficient

One of the key parameters for Bragg grating (and in particular for DFB lasers) is the coupling coefficient, which describes the degree to which oppositely propagating modes transfer energy; this has been calculated analytically or numerically in DFB lasers, using the coupling mode theory in different shapes [12], [13]. In our case, the teeth shape is very different from that used in conventional DFB lasers.

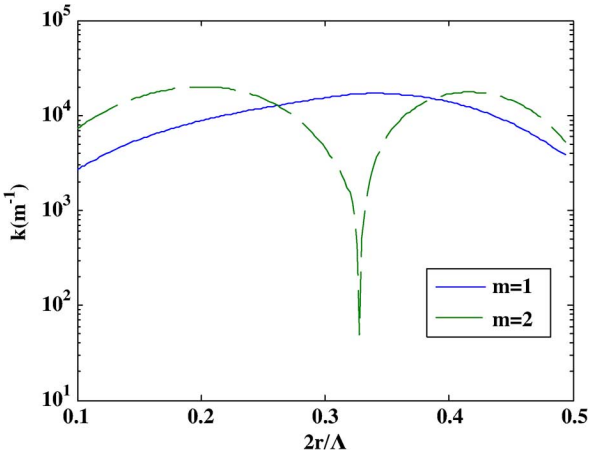

Fig. 3. Coupling coefficient k versus of the ratio between the tooth height $(2r)$ and grating period Λ at $D = 1$ μm and $d = 1$ μm for different m, $m = 1$ (solid line) and $m = 2$ (dashed line).

In the grating region, $g_1 < x < g_2$, the refractive index variation is

$$\Delta\left[n^2(x,y,z)\right] = \begin{cases} n_1^2 - n_2^2, & \text{in area A} \\ n_2^2 - n_1^2, & \text{in area B.} \end{cases} \tag{2}$$

The coupling coefficient produced by corrugations can be expressed as [12], [13] $k = (k_0^2/2\beta)\int\int_{\text{corrugation}} \Delta[n^2(x,y,z)]E^2 dxdy$, where E is the normalized field. This yields to [12]

$$\begin{aligned} k = {} & \frac{-ik_0^2\left(n_1^2 - n_2^2\right)}{4\pi m\beta N^2} \\ & \times \left\{ \int_{-\infty}^{+\infty}\int_{g_0}^{g_2} \left\{ \exp\left[\frac{i2\pi m w_2(x)}{\Lambda}\right] \right.\right. \\ & \left. - \exp\left[\frac{i2\pi m w_1(x)}{\Lambda}\right] \right\} E^2(x,y)dxdy \\ & - \int_{-\infty}^{+\infty}\int_{g1}^{g_2} \left\{ \exp\left[\frac{i2\pi m w_4(x)}{\Lambda}\right] \right. \\ & \left.\left. - \exp\left[\frac{i2\pi m w_3(x)}{\Lambda}\right] \right\} E^2(x,y)dxdy \right\} \end{aligned}$$

where m is the Bragg scattering order. The propagation constant β, and the electrical field E all depend on the unperturbed geometry, i.e., n_1, n_2, n_3, n_4 (Fig. 1), as well as the transverse mode number. Fig. 3 shows plots of the coupling coefficient k versus the ratio between the tooth height $(2r)$ and the period Λ at $m = 1$ and 2. Here the microfiber diameter is $D = 1$ μm, $d = 1$ μm, $n_1 = 1$, $n_2 = n_3 = 1.46$, $n_4 = 1.375$, $\Lambda = 1.12$ μm, and $\lambda = 1550$ nm. The mode fields are obtained from simulations with the commercial finite-element software Comsol

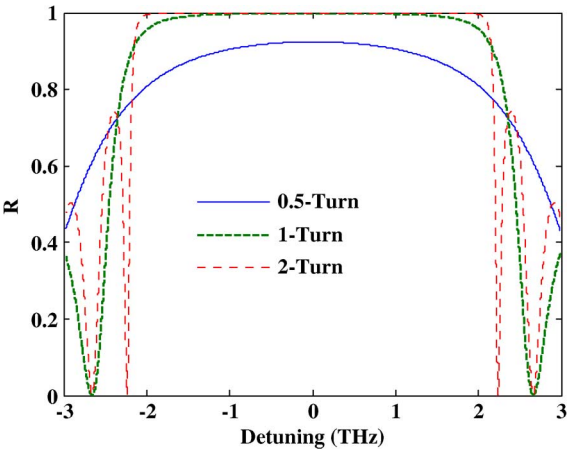

Fig. 4. Reflection spectra versus frequency detuning in uniform gratings for 0.5-turns (solid line), 1-turn (dashed line), and 2-turns (dotted line) with $k = 10^4$ m^{-1}.

Multiphysics. The coupling coefficient is tens of mm^{-1}. Interestingly, k is strongly dependent on the tooth depth and the microfiber diameter, but it always shows a maximum for $m = 1$ and a minimum for $m = 2$ at $2r/\Lambda \approx 0.32$. This can be ascribed to the dependence of k on d' and the corrugation area, and d' achieves maximum at $r = \Lambda/\pi$. In practical applications, it is convenient to use $m = 2$ with larger pitch.

IV. Reflection

Since the number of periods per turn increases with the rod diameter, a larger number of holes means larger capillaries: this implies an increased difficulty in manufacture and, for practical application, it should be better to use a rod with a diameter of several hundred micrometers.

For a 250-μm-diameter rod, the number of periods in one turn is about 700, and increases linearly with the number of turns. The power reflectivity is given by

$$R = \frac{\sinh\left(k^2 - (n_{\text{eff}}\delta\omega/c)^2\right)}{\cosh\left(k^2 - (n_{\text{eff}}\delta\omega/c)^2\right) - (n_{\text{eff}}\delta\omega/ck)^2}$$

where $c = 3 \times 10^8$ m/s, L is the contact length between microfiber and support rod, and $\delta\sigma$ is the detuning from the center frequency. Typical examples of the power reflectivity for uniform gratings in 0.5-turn, 1-turn, and 2-turn with $k = 10^4$ m^{-1} are shown in Fig. 4, plotted versus the frequency detuning. Broadband peaks with reflectivities close to 100% can be easily achieved for a two-turn MGB.

If the microfiber is not perpendicular to the rod and crosses it at an angle θ, the Bragg condition (1) is expressed as [13], $\lambda_B = 2n_{\text{eff}}(\Lambda/cos\theta)/m$.

By changing θ gradually, the Bragg wavelength will also change gradually; thus it is possible to get a chirped broadband grating, and to control the grating Bragg wavelength by controlling the angle at which the microfiber approaches the microstructured rod. Moreover, it is also possible to realize wideband gratings by varying Λ or r with varying β.

The use of microstructured support rods to make gratings provides an extreme flexibility because it is easier to be dealt with than the microfiber. By controlling the air holes' geometry, it is possible to get several-layer corrugations or phase-shifted gratings. If the rod is coated with an active layer or the holes are filled with an active medium, it generates a laser. If holes are used as microfluidic channels, the support rod can work as a sensor. Moreover, since only a very short piece of rod is needed for each device, the average device cost is very low. Devices can be coated with stable polymers such as Teflon and UV375, and maintain the extraordinary strength they exhibit as manufactured [2]. Moreover, since they are fabricated from a tapered single-mode fiber, they maintain the original size at their input–outputs, minimizing the insertion loss.

V. Conclusion

We have presented the schematic on the realization of a micrograting by wrapping a microfiber on a microstructured rod, which has deep teeth and large coupling coefficient. Different grating profiles can be realized by changing the approach angle between microfiber and rod or by designing and fabricating rods with different geometries. Microfiber gratings have a great potential for future all-fiber microcircuits: in principle, they allow reproduction on a microscopic scale of all grating-based devices and sensors previously realized in conventional optical fibers.

References

[1] G. Brambilla, F. Xu, and X. Feng, "Fabrication of optical fibre nanowires and their optical and mechanical characterisation," *Electron. Lett.*, vol. 42, pp. 517–519, Apr. 27, 2006.

[2] G. Brambilla, F. Xu, P. Horak, Y. Jung, F. Koizumi, N. P. Sessions, E. Koukharenko, X. Feng, G. S. Murugan, J. S. Wilkinson, and D. J. Richardson, "Optical fiber nanowires and microwires: Fabrication and applications," *Adv. Opt. Photon.*, vol. 1, pp. 107–161, 2009.

[3] F. Xu and G. Brambilla, "Embedding optical microfiber coil resonators in Teflon," *Opt. Lett.*, vol. 32, pp. 2164–2166, Jul. 2007.

[4] M. Sumetsky, "Demonstration of a multi-turn microfiber coil resonator," in *Proc. Optical Fiber Communication Conf.*, San Diego, CA, 2007.

[5] F. Xu and G. Brambilla, "Demonstration of a refractometric sensor based on optical microfiber coil resonator," *Appl. Phys. Lett.*, vol. 92, p. 101126-3, 2008.

[6] F. Xu, P. Horak, and G. Brambilla, "Optical microfiber coil resonator refractometric sensor," *Opt. Express*, vol. 15, pp. 7888–7893, 2007.

[7] W. Ding, S. R. Andrews, T. A. Birks, and S. A. Maier, "Modal coupling in fiber tapers decorated with metallic surface gratings," *Opt. Lett.*, vol. 31, pp. 2556–2558, 2006.

[8] V. Hodzic, J. Orloff, and C. C. Davis, "Periodic structures on biconically tapered optical fibers using ion beam milling and boron implantation," *J. Lightw. Technol.*, vol. 22, no. 6, pp. 1610–1614, Jun. 2004.

[9] W. Ding, S. R. Andrews, and S. A. Maier, "Surface corrugation Bragg gratings on optical fiber tapers created via plasma etch postprocessing," *Opt. Lett.*, vol. 32, pp. 2499–2501, 2007.

[10] J. C. Knight, "Photonic crystal fibres," *Nature*, vol. 424, pp. 847–851, 2003.

[11] M. Bayindir, F. Sorin, A. F. Abouraddy, J. Viens, S. D. Hart, J. D. Joannopoulos, and Y. Fink, "Metal-insulator-semiconductor optoelectronic fibres," *Nature*, vol. 431, pp. 826–829, 2004.

[12] W. Streifer, D. Scifres, and R. Burnham, "Coupling coefficients for distributed feedback single- and double-heterostructure diode lasers," *IEEE J. Quantum Electron.*, vol. 11, no. 11, pp. 867–873, Nov. 1975.

[13] W. Streifer and A. Hardy, "Analysis of two-dimensional waveguides with misaligned or curved gratings," *IEEE J. Quantum Electron.*, vol. 14, no. 12, pp. 935–943, Dec. 1978.